

CrossMark  
click for updatesCite this: *RSC Adv.*, 2015, 5, 83818

## New properties in old systems: cooperative electric order in ferrocene and ammonia-borane†

J. M. Bermúdez-García,<sup>a</sup> S. Yáñez-Vilar,<sup>ab</sup> S. Castro-García,<sup>a</sup> M. A. Señaris-Rodríguez<sup>a</sup> and M. Sánchez-Andújar<sup>\*a</sup>

After half a century of intensive and extensive studies on ferrocene [Fe(C<sub>5</sub>H<sub>5</sub>)<sub>2</sub>] and ammonia-borane (H<sub>3</sub>N·BH<sub>3</sub>), it is very exciting to observe that these “classical” compounds still hide interesting properties never described before. Despite it being well-known that they both experience phase transitions as a function of temperature, here, for the first time, we give experimental evidence for the dielectric transitions they experience associated to the former, results that we support with DFT calculations. In that context, we report that ferrocene displays a temperature-induced paraelectric to antiferroelectric transition associated with the monoclinic–triclinic transition, which implies order–disorder of the cyclopentadienyl (Cp) ligands and displacement of the Fe atoms within the ferrocene molecules. As for the ammonia-borane, we report a sharp dielectric transition at  $T \approx 232$  K, associated with a structural transition that combines ordering and atomic displacement of the H<sub>3</sub>N·BH<sub>3</sub> molecules. In this case, we attribute such behaviour to the temperature dependent displacement of the H<sub>3</sub>N·BH<sub>3</sub> molecules out-of the crystal polar *c*-axis.

Received 28th June 2015  
Accepted 28th September 2015

DOI: 10.1039/c5ra12506e

www.rsc.org/advances

### Introduction

Solids are known to undergo a variety of phase transitions accompanied by significant changes in some of the properties. Therefore, the study of structural transitions, as well as their implications, is of major interest to scientists working in very diverse areas, ranging from theoretical physics and chemistry to materials technology.

Typical examples of phase transitions that play a major role in driving a function to a material are those involving changes in magnetic, electrical and dielectric properties.<sup>1</sup> Within this latter, those leading to cooperative electric order (specially ferro- or ferri-electric dipole arrangements) attract great attention because of the significant applications of the resulting materials in electric and electronic devices, such as capacitors, temperature sensors, data storage memories, mechanical actuators, and so on.<sup>2</sup>

In that context, two main types of phase transitions are known to be the underlying cause for the appearance of cooperative electric ordering in some solids, namely displacive and order–disorder transitions<sup>3</sup> even if they often appear associated.<sup>4</sup>

Various approaches have been developed to prepare novel materials with phase transition-induced dielectric properties. Among them, the search for solid compounds in which freezing and reorientation of polar molecules and/or ionic groups can occur and easily lead to phase transitions and associated cooperative electric order. In this context, the organic–inorganic hybrid compounds also known as metal–organic frameworks (MOFs)<sup>2</sup> and molecular solids have been recently claimed to be excellent candidates to show phase transition behaviours,<sup>5</sup> even if their behaviours have been much less explored than that of other non-molecular solids. And very outstanding ferroelectric (and even multiferroic) materials have already been discovered among the former, such as (DMA)[Mn(HCOO)<sub>3</sub>] (where DMA is the dimethylammonium cation).<sup>6,7</sup>

In this paper, we focus on the family of molecular solids to illustrate and emphasize the important role of phase transitions on the properties of “old” compounds, albeit with new properties, belonging to this category.

For this purpose, we revisit two very famous “classical” molecular compounds, such as ferrocene, bis(cyclopentadienyl) iron, [Fe(C<sub>5</sub>H<sub>5</sub>)<sub>2</sub>] and ammonia-borane (H<sub>3</sub>N·BH<sub>3</sub>). These compounds are known to experience phase transitions as a function of temperature, and their structural characteristics render them good candidates to display interesting dielectric behaviour even if such structure–property relationship has up to now remained unexplored.

As for the first of these compounds, since its discovery in 1951 the impact of such breakthrough and pioneering work has been enormous.<sup>8</sup> Ferrocene opened new areas of chemistry,

<sup>a</sup>QuiMolMat Group, Department of Fundamental Chemistry, Faculty of Science and CICA, University of A Coruña, Campus A Coruña, 15071 A Coruña, Spain. E-mail: msanchez@udc.es

<sup>b</sup>Department of Applied Physics, University of Santiago de Compostela, 15782 Santiago de Compostela, Spain

† Electronic supplementary information (ESI) available: Scheme of temperature and pressure phase transitions of ammonia-borane. See DOI: 10.1039/c5ra12506e



deepened our understanding of structure, bonding, and reactivity, and paved the way for the burgeoning field of organometallic chemistry itself.<sup>9</sup>

It is well-known that ferrocene displays an order-disorder/displacive phase transition at  $T_t \approx 164$  K. From the structural point of view, this phase transition involves two different crystalline polymorphs:<sup>10</sup> the orange high temperature HT-phase (monoclinic) and the canary-yellow low-temperature LT-phase (triclinic). The first of them, that is also the room temperature polymorph, is monoclinic with space group  $P2_1/a$ ,  $Z = 2$ . It contains only one type of centrosymmetric ferrocene molecules, that is the basis for the centrosymmetric staggered molecular structure<sup>11</sup> usually shown in textbooks (Fig. 1a). Nevertheless, the apparent centrosymmetry of the ferrocene molecule is not a genuine molecular property, but the result of the statistical distribution of the cyclopentadienyl (Cp) ring orientations into the averaged structure (dynamically disordered). In fact, ferrocene is an artificial molecular rotor,<sup>12</sup> being perhaps the simplest type of molecular carousel, a compound consisting of two or more planar (or nearly planar) “decks” which rotate and remain parallel to each other.

Below  $T_t \approx 164$  K, the rotation of the Cp rings gets frozen<sup>13</sup> and the ferrocene crystals become triclinic (space group  $F\bar{1}$ ,  $Z = 16$ ). The resulting LT-phase is closely related to the HT-phase one, but it presents two main differences respect to the HT-phase: (i) the ferrocene Cp rings adopt an almost eclipsed conformation ( $\alpha \approx 9^\circ$ ) (Fig. 1b), and (ii) there are two slightly distinct types of non-centrosymmetric ferrocene molecules,<sup>14</sup> (we will come back to this point in the “Results and discussion” section).

In relation to the second compound, ammonia-borane is a white crystalline solid that was first prepared in 1955.<sup>15</sup> This compound is presented in almost all chemistry textbooks as an example of a Lewis acid/base adduct<sup>16</sup> and more recently it is attracting increased attention in view of its potential as a hydrogen storage material.<sup>17</sup>

The ammonia-borane displays an order-disorder/displacive phase transition at  $T_t \approx 225$  K. From the structural point of view, ammonia-borane can adopt two different crystal structures at ambient pressure both of which are non-centrosymmetric: the tetragonal high temperature HT-phase with space group  $I4mm$ <sup>18–20</sup> and the orthorhombic low temperature LT-phase with space

group  $Pmn2_1$ , see Fig. 2. In the HT-phase, the  $H_3N \cdot BH_3$  molecules are collinear to the  $c$ -axis and the H-atoms are disordered over different crystallographic sites.<sup>21</sup> On cooling below  $T_t \approx 225$  K the ammonia-borane crystals become orthorhombic. In contrast with the HT-polymorph, in this LT-structure the  $H_3N \cdot BH_3$  molecules are alternatively tilted along the  $c$ -axis and the H-atoms are ordered in a single crystallographic site, see Fig. 2.

Despite extensive and intense studies on ferrocene and ammonia-borane in many different contexts, very little attention has been paid to their dipole moment structure and associated dielectric response. In that context, just Gaffar *et al.*<sup>22</sup> published a paper about the influence of  $\gamma$ -radiation on the electric and dielectric properties of ferrocene. However, this study had focused mainly on the former and just briefly makes reference to a weak dielectric anomaly associated to the order-disorder transition, without analysing its origin and implications. As for the ammonia-borane, to the best of our knowledge there are no previous studies that refer to its dielectric behaviour.

In the present work, we give experimental evidence of the dielectric response of both ferrocene and ammonia-borane and we use DFT calculations to justify their dipolar structures. Remarkably, we discover a dielectric transition associated to a phase transition in both inorganic compounds. We rationalize the obtained results on the basis of structure-properties relationships, which we establish taking into account their dipole moment distributions, and that we calculate using reported crystal data.

## Results and discussion

### Ferrocene

Fig. 3 shows the temperature dependence of the real part of the complex dielectric permittivity (the so-called dielectric constant)  $\epsilon'_r$  of ferrocene measured upon heating and cooling the sample. Very interestingly, in both types of experiments, the  $\epsilon'_r$  vs. temperature curve displays a small and broad peak, that is seen to occur at  $T_{\text{heat}} \approx 195$  K on heating, and at  $T_{\text{cool}} \approx 175$  K on cooling.

Such features are fully reproducible and can not be attributed to the experimental error of the measurement. These

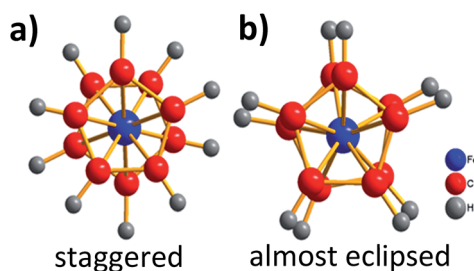


Fig. 1 Representations of the two different molecular conformations of ferrocene presented in the two crystalline polymorphs of this compound: (a) staggered (monoclinic HT-phase) and (b) almost eclipsed (triclinic LT-phase).

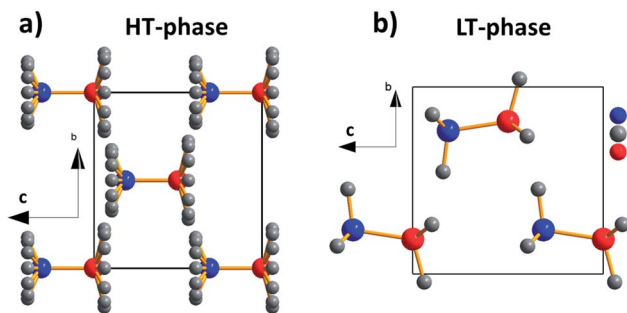


Fig. 2 Crystal structure of the ammonia-borane polymorphs: (a) HT-phase with H-atoms disordered and the molecules collinear to the  $c$ -axis and (b) LT-phase with H-atoms ordered and the molecules tilted along the  $c$ -axis.



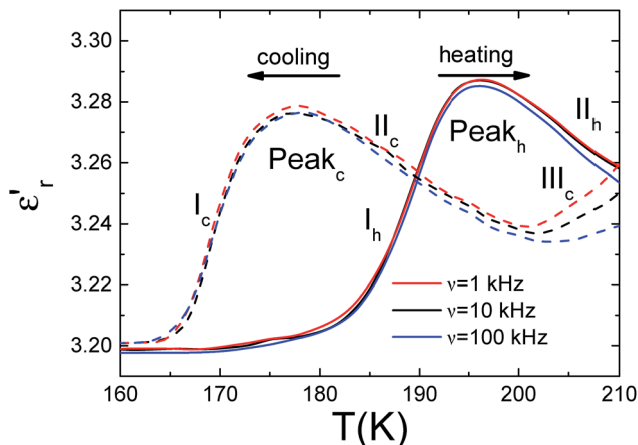


Fig. 3 Temperature dependence of the dielectric constant of ferrocene, measured at different frequencies upon heating (solid lines) and cooling (dash lines). The presence of a broad maximum at the transition temperature, either  $T_{\text{cool}}$  or  $T_{\text{heat}}$ , is highlighted and the roman numbers (with the corresponding subscript "h" for heating and "c" for cooling) are labels for regions with different dielectric behaviours (see text).

anomalies in the dielectric constant occur close to the temperature reported for the phase transition, which according to differential scanning calorimetry (DSC) measurements take place on cooling at  $T_{\text{cool}} \approx 169$  K and  $\approx 164$  K.<sup>23</sup>

Also, the observed thermal hysteresis is characteristic of a first-order transition.<sup>6</sup>

In addition, for temperatures higher than  $T_t$  (region II in Fig. 3),  $\epsilon'_r$  is seen to decrease as temperature increases further following the typical trend of a paraelectric behaviour. Meanwhile the drop below  $T_t$  (region I) resembles a paraelectric-antiferroelectric transition.

It should be noted that in these two regions the dielectric response is purely intrinsic of the bulk of the material, as confirmed by impedance complex plane analysis of the obtained data (Fig. S1, ESI†).

In addition to this intrinsic behaviour, an extrinsic one is observed for higher temperatures, region III ( $T > 200$  K on cooling and  $T > 215$  K on heating) that gives rise to a new rise in  $\epsilon'_r$  as temperature increases.

With the aim of understanding the intrinsic dielectric response of the ferrocene, we have further explored the characteristics of the low and high temperature phases, paying special attention to the distribution of the associated dipole moments, as obtained from the DFT calculations.

In the HT-phase, where the ferrocene molecules are centrosymmetric, the only possible origin for dipole moments are the cyclopentadienyl ligands, that carry a very weak dipole moment of  $\mu = 0.006$  D.

Nevertheless, as in this HT-phase the Cp rings have a "free" rotation movement around the iron axle, their associated dipole moment gets averaged out.

Meanwhile, in the LT-phase the situation is much more complex. As indicated before, in this polymorph there are two slightly different types of ferrocene molecules<sup>14</sup> (hereafter

named as I and II). Their main differences rely in the rotation angle of the two Cp ligands and the position of the Fe atoms inside the Cp<sub>2</sub> sandwich.<sup>14</sup> In any case both types of ferrocene molecules are non-centrosymmetric as the Fe-atoms are off-center shifted from the inversion center of the sandwich. The calculated dipole moment associated to these ferrocene molecules is small, even if one order of magnitude higher than in the case of the Cp ligand; and its value in molecules type I is almost twice as high as that displayed by molecules type II:  $\mu_{\text{tricl-I}} = 0.082$  D versus  $\mu_{\text{tricl-II}} = 0.043$  D. Moreover, according to the calculations the orientation of their corresponding dipole moments also differs: in the case of the ferrocene molecules type I, the associated dipole is arranged parallel to the two cyclopentadienyl rings (see Fig. 4a), while in the ferrocene molecules type II it is arranged towards one of the cyclopentadienyl rings (see Fig. 4b).

The peculiar arrangement of both types of ferrocene molecules within the LT-crystal structure yields to a cooperative antiferroelectric arrangement of dipole moments, where all the dipoles get cancelled out in the unit cell, as sketched in Fig. 5.

With all this information in mind, we can rationalize the dielectric response of ferrocene as follows:

The observed paraelectric behaviour for  $T > 190$  K is due to the fact that at those temperatures the Cp ligands are not static but are rotating, as thermal energy is high enough to allow for such a process. As a consequence, the electrical dipoles associated to the ferrocene molecules will average in different directions upon rotation and account for the observed paraelectric behaviour. As temperature decreases, the speed of rotation of the cyclopentadienyl rings slows down and, as a consequence,  $\epsilon'_r$  increases.

At around  $T_t \approx 164$  K, the order-disorder transition associated to the freezing of the molecular rotation of the Cp ligands takes place: below that temperature the Cp rings can no longer rotate and have their positions fixed within the ferrocene molecules. Simultaneously, the Fe atoms experience an off-center shift within the Cp<sub>2</sub> sandwiches, while the relative distribution of the ferrocene molecules is preserved, and a change in the symmetry of the crystal occurs.

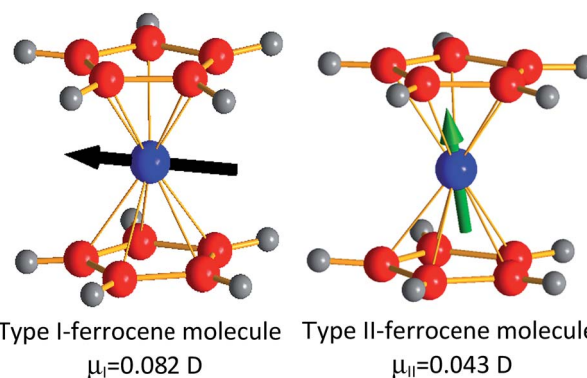


Fig. 4 Representations of the two types of ferrocene molecules present in the LT-phase. The arrows represent the electrical dipole moments (not drawn to scale) of these molecules.



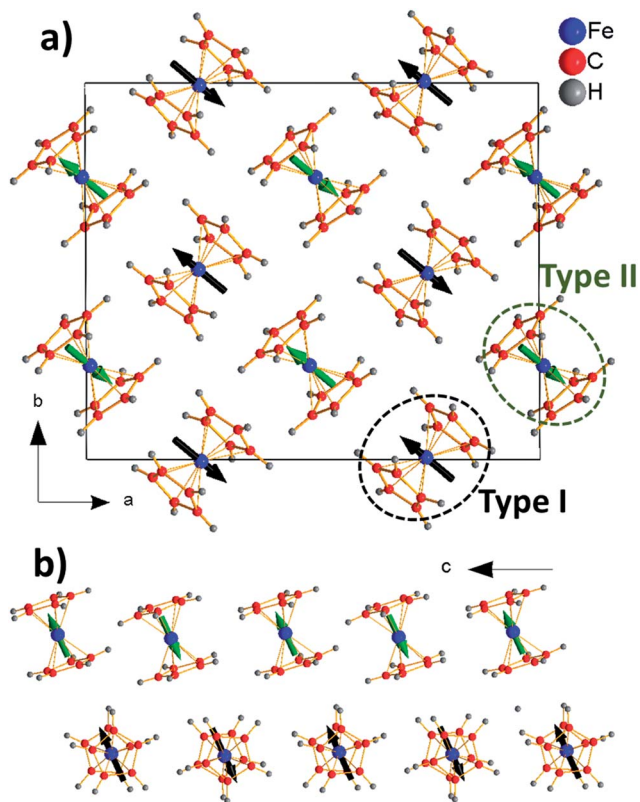


Fig. 5 Dipole distribution in the triclinic LT-phase of ferrocene: (a) within the  $ab$ -plane and (b) along the  $c$ -axis. Arrows represent the electric dipole moment of the ferrocene molecules (black for molecules type I and green molecules type II).

Even more, the off-center shift of the Fe atoms within the molecules is cooperative, and results in a global compensation of their associated electric dipoles. This gives rise to a drop in the dielectric constant, which signals the occurrence of the corresponding paraelectric–antiferroelectric transition.

Nevertheless, as the values of the electric dipole moment of the ferrocene molecules are low, the observed dielectric anomaly is much smaller than in the case of other antiferroelectric materials.<sup>3</sup>

Finally, we attribute the rise in  $\epsilon'_r$  in region III to the presence of extrinsic effects, such as moisture molecules at the surface of the measured pellet, that the higher the temperature the more significantly contribute to the signal in that temperature interval. A similar feature has been observed, for example, in the recently studied hybrid organic–inorganic compounds with perovskite-like structure of general formula  $(\text{DMA})[\text{M}(\text{HCOO})_3]$  ( $\text{M}^{2+} = \text{Mg}^{2+}, \text{Mn}^{2+}, \text{Fe}^{2+}, \text{Co}^{2+}, \text{Ni}^{2+}$  and  $\text{Zn}^{2+}$ ) exhibiting dielectric transitions.<sup>6,7</sup>

### Ammonia-borane

Fig. 6 shows the temperature dependence of the real part of the complex dielectric permittivity  $\epsilon'_r$  of ammonia-borane. Very interestingly, the  $\epsilon'_r$  versus temperature curve displays a sharp kink around  $T \approx 232$  K, close to the temperature reported for the structural transition as seen by DSC measurements.<sup>24</sup> As it

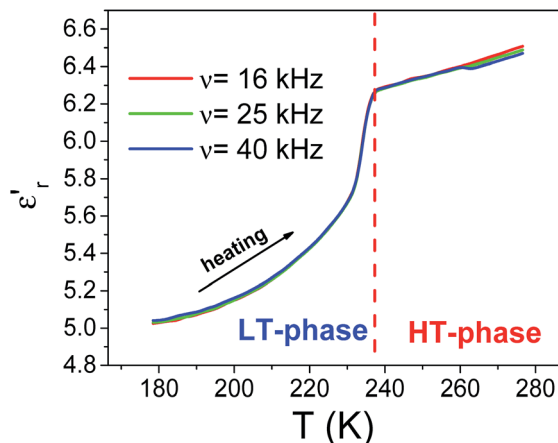


Fig. 6 Dielectric constant of ammonia-borane as a function of temperature measured at different frequencies.

can be observed  $\epsilon'_r$  is frequency independent and increases with temperature in the whole studied temperature range. Another interesting remark is the almost linear behaviour of  $\epsilon'_r(T)$  for  $T > 232$  K.

To further deepen in the origin of the observed dielectric transition, we focus again our attention on the dipole moment associated to the molecules and their distribution within the crystal. We have calculated an electric dipole moment of  $\mu \approx 5.67$  D associated to the ammonia-borane molecules, which is collinear to the molecule axis. To estimate their distribution in the crystal, we have examined closely their contribution along the  $c$ -axis, taking into account that both polymorphs, LT-phase (orthorhombic) and HT-phase (tetragonal), display non-centrosymmetric space groups with a unique polar direction along the  $c$ -axis, (by symmetry the dipole is not cancelled uniquely along the  $c$ -axis). In the HT-phase, the  $\text{H}_3\text{N} \cdot \text{BH}_3$  molecules are collinear with the  $c$ -axis, and so are the associated electric dipole moments (see Fig. 7a). The parallel arrangement of the dipoles gives rise to a net polarization that accounts for the higher values of the dielectric constant for  $T > 240$  K. Meanwhile, in the LT-phase (see Fig. 7b), the molecule arrangement becomes buckled and the molecules are slightly inclined along the polar  $c$ -axis.

Since the material polarization comes exclusively from the component of the dipole moments along the  $c$ -axis, the effective net value gets reduced as a function of these dipole moments shift. Therefore, such contribution is related to the tilting of the  $\text{H}_3\text{N} \cdot \text{BH}_3$  molecules out-of the polar  $c$ -axis, so that the larger is this tilting the smaller becomes the resulting dielectric constant, see Fig. S2 of ESI.†

In that context, it is known that in this LT-phase the angle between the molecules and the polar  $c$ -axis increases upon cooling (from  $18^\circ$  at 200 K (ref. 19) to  $26^\circ$  at 90 K (ref. 21)). That is the reason why the dielectric constant—that has already dropped as compared to the HT-phase—continues to decrease further as the temperature is reduced.

In view of the obtained results, we attribute the observed rather sharp jump in the dielectric constant as a function of temperature to the transition between two ordered phases with



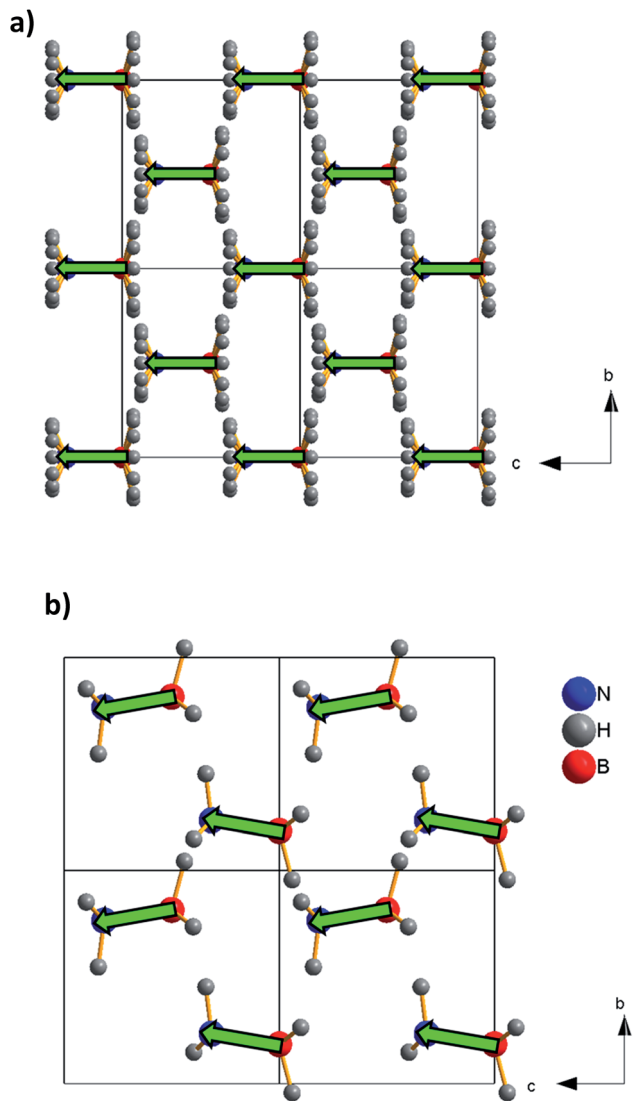


Fig. 7 Dipole distribution in the two polymorphs of ammonia-borane viewed along [100] direction: (a) tetragonal HT-phase and (b) orthorhombic LT-phase, where the green arrows represent the electric dipole moment of the ammonia-borane molecules. We have expanded the number of unit cells to facilitate the visualization of the dipoles arrangement.

the different ferroelectric arrangements described above. Hence, the order-disorder process of the H-atoms of the  $\text{H}_3\text{N}\cdot\text{BH}_3$  molecules seem to be not significant for the reported dielectric anomaly.

Nevertheless, and despite such ferroelectric arrangements, ammonia-borane cannot be catalogued as a ferroelectric material. By definition this would mean that its polarization can be reversed by an applied external electric field. In this case, it is not possible because it would imply the rotation of all  $\text{H}_3\text{N}\cdot\text{BH}_3$  molecules within the crystal by very large angles, up to  $180^\circ$ .

Finally, taking into account the here obtained findings, we propose that the ammonia-borane could display a huge dielectric transition induced by external pressure. In this context, Filinchuk *et al.*<sup>25</sup> have recently reported the structural evolution of this compound under external pressure using

synchrotron powder diffraction. These authors have observed that this compound displays a reversibly phase transition, from the disordered HT-tetragonal phase to a new ordered phase (S.G.:  $Cmc2_1$ ), phase transition that at room temperature takes place at around 1.2 GPa. In such high-pressure  $Cmc2_1$  polymorph, the tilting of the  $\text{H}_3\text{N}\cdot\text{BH}_3$  molecules with respect to the *c*-axis is very large ( $69^\circ$  at 1.2 GPa and even up to  $79^\circ$  at 4.65 GPa), much larger than in the LT-orthorhombic phase.

Therefore, on the basis of the here presented results, we propose that external pressure will induce a transition from a ferroelectric arrangement of the electric dipoles to an almost antiferroelectric arrangement, so that the anomalies in the dielectric constant as a function of pressure should be much more pronounced than the here reported as a function of temperature.

Therefore, taking into account the characteristics of this compound, we propose that it would be used also as a sensitive pressure dielectric material.

## Experimental

### Materials

Ferrocene (98%, Aldrich) and ammonia-borane (97%, Aldrich) were commercially available and used as purchased without further purification.

### Dielectric properties

The complex dielectric permittivity ( $\epsilon_r = \epsilon'_r - \epsilon''_r$ ) of the cold-press pelletized samples was measured as a function of frequency and temperature with a parallel-plate capacitor coupled to a Solartron 1260A Impedance/Gain-Phase Analyzer, capable to measure in the frequency range from 10  $\mu\text{Hz}$  up to 32 MHz with an accuracy of 0.1% using an amplitude of 2 V. The capacitor was mounted in a Janis SVT200T cryostat refrigerated with liquid nitrogen, and with a Lakeshore 332 incorporated to control the temperature from 78 K up to 400 K. The data were collected on heating and cooling and before carrying out the measurements, the pellets were kept for two minutes at each temperature so as to reach the thermal equilibrium. The impedance analysis software SMART (Solartron Analytical) was used for data acquisition and processing. Impedance complex plane plots were analyzed using the LEVM program, a particular program for complex nonlinear least squares fitting.<sup>26</sup>

Pelletized samples made out of cold-press non-oriented single crystal with an area of approximately  $530 \text{ mm}^2$  and a thickness of approximately 1 mm were prepared to fit into the capacitor, and silver paste was painted on their surfaces to ensure a good electrical contact with the electrodes.

All the dielectric measurements were carried out in a nitrogen atmosphere where several cycles of vacuum and nitrogen gas were performed to ensure that the sample environment is free of water.

Attempts to directly measure single crystals failed, as these break into powder at the phase transition.

### Quantum calculations

All the values for the calculation of the electric dipole moments presented in this work were performed employing the Gaussian



09 package (Revision D.01).<sup>27</sup> Single point energy calculations were performed employing DFT within the hybrid-GGA (generalized gradient approximation) with the B3LYP exchange-correlation functional. Input geometries were generated from the crystallographic data of ferrocene<sup>14</sup> and of ammonia-borane<sup>19,28</sup> reported at the literature. The standard 6-31+G(d) basis set was used throughout this work for non-metallic atoms and TZVP (5d,7f)-valence triple-zeta plus polarization basis set was used for iron atoms.

## Conclusions

In this work we show experimental studies of the solid state dielectric response of two very famous “classical” molecular inorganic compounds, namely ferrocene and ammonia-borane. Remarkably, both compounds display a dielectric transition associated to the structural phase transition as a function of temperature, which emphasizes the important role of order-disorder/displacive phase transitions on the dielectric properties.

We rationalize the obtained results on the basis of structure properties relationships, which we establish taking into account their dipole moment distributions, that we have calculated by means of quantum calculations using reported crystal data.

As shown, ferrocene displays a temperature-induced paraelectric to antiferroelectric transition associated to a phase transition that implies order-disorder of the Cp ligands and displacement of the Fe atoms within the ferrocene molecules. We rationalize the obtained results on the basis of a complex antiferroelectric arrangement of the electric dipole moments (induced by the displacement of the Fe atoms) in the LT-phase. Such arrangement gets destroyed as  $T$  increases above  $T_t$ : the ferrocene molecules become centrosymmetric and the dipole moments associated to the Cp rings become averaged as a result of their rotation.

On the other hand, we show that ammonia-borane displays a sharp dielectric transition at  $T \approx 232$  K, associated to a structural transition that combines ordering and atomic displacement mechanisms of the  $H_3N \cdot BH_3$  molecules. In this case, we attribute such behaviour to the temperature dependent displacement of the  $H_3N \cdot BH_3$  molecules out-of the crystal polar  $c$ -axis. Above  $T_t$ , this compound exhibits a relative high polarization related to the collinear dipole moments, which lie parallel to  $c$ -axis. Meanwhile below  $T_t$ , the dipole moments display a shift out of  $c$ -axis, resulting in a polarization decrease. Additionally, we propose that external pressure will induce a transition from a ferroelectric to an almost antiferroelectric dipole arrangement.

These findings demonstrate that both ferrocene and ammonia-borane compounds are sensitive thermoresponsive dielectric materials, result that opens up new possibilities for their potential “novel” applications in a wide variety of fields, such as electronic materials.

## Acknowledgements

The authors are grateful for financial support from Ministerio de Economía y Competitividad (MINECO) ENE2014-56237-C4-4-

R and Xunta de Galicia under the project GRC2014/042. The authors are indebted to Centro de Supercomputación de Galicia (CESGA) for providing the computer facilities. S. Y.-V. acknowledges Xunta de Galicia for a Postdoctoral fellowship.

## Notes and references

- 1 C. N. R. Rao and J. Gopalakrishnan, in *New Directions in Solid State Chemistry*, Cambridge University Press, 1997.
- 2 W. Zhang and R. G. Xiong, *Chem. Rev.*, 2012, **112**, 1163.
- 3 M. E. Lines and A. M. Glass, in *Principles applications of ferroelectric and related materials*, Oxford University Press, New York, 2001.
- 4 A. Bussmann-Holder and N. Dalal, *Struct. Bonding*, 2007, **124**, 1.
- 5 A. B. Cairns and A. L. Goodwin, *Chem. Soc. Rev.*, 2013, **42**, 4881.
- 6 (a) P. Jain, N. S. Dalal, B. H. Toby, H. W. Kroto and A. K. Cheetham, *J. Am. Chem. Soc.*, 2008, **130**, 10450; (b) P. Jain, V. Ramachandran, R. J. Clark, H. D. Zhou, B. H. Toby, N. S. Dalal, H. W. Kroto and A. K. Cheetham, *J. Am. Chem. Soc.*, 2009, **131**, 13625.
- 7 M. Sánchez-Andújar, S. Presedo, S. Yáñez-Vilar, S. Castro-García, J. Shamir and M. A. Señaris-Rodríguez, *Inorg. Chem.*, 2010, **49**, 1510.
- 8 T. J. Kealy and P. L. Pauson, *Nature*, 1951, **168**, 1039.
- 9 K. Heinze and H. Lang, *Organometallics*, 2013, **32**, 5623.
- 10 J. D. Dunitz, *Acta Crystallogr., Sect. B: Struct. Sci.*, 1995, **51**, 619.
- 11 J. D. Dunitz, L. E. Orgel and A. Rich, *Acta Crystallogr.*, 1956, **9**, 373.
- 12 G. S. Kottas, L. I. Clarke, D. Horinek and J. Michl, *Chem. Rev.*, 2005, **105**, 1281.
- 13 J. W. Edwards, L. Kington and R. Mason, *Trans. Faraday Soc.*, 1960, **56**, 660.
- 14 P. Seiler and J. D. Dunitz, *Acta Crystallogr., Sect. B: Struct. Crystallogr. Cryst. Chem.*, 1979, **35**, 2020.
- 15 S. G. Shore and R. W. Parry, *J. Am. Chem. Soc.*, 1955, **77**, 6084.
- 16 H. Li, Q. Yang, X. Chen and S. G. Shore, *J. Organomet. Chem.*, 2014, **751**, 60.
- 17 A. Staubitz, A. P. M. Robertson and I. Manners, *Chem. Rev.*, 2010, **110**, 4079.
- 18 S. G. Shore, *J. Am. Chem. Soc.*, 1965, **4**, 8.
- 19 W. T. Klooster, T. F. Koetzle, P. E. M. Siegbahn, T. B. Richardson and R. H. Crabtree, *J. Am. Chem. Soc.*, 1999, **121**, 6338.
- 20 N. J. Hess, G. K. Schenter, M. R. Hartman, L. L. Daemen, T. Proffen, S. M. Kathmann, C. J. Mundy, M. Hartl, D. J. Heldebrant, A. C. Stowe and T. Autrey, *J. Phys. Chem. A*, 2009, **113**, 5723.
- 21 M. E. Bowden, G. J. Gainsford and W. T. Robinson, *Aust. J. Chem.*, 2007, **60**, 149.
- 22 M. A. Gaffar and A. G. Hussien, *J. Phys. Chem. Solids*, 2011, **62**, 2011.
- 23 K. Ogasahara, M. Sorai and H. Suga, *Mol. Cryst. Liq. Cryst.*, 1981, **71**, 189.
- 24 O. Palumbo, A. Paolone, P. Rspoli, R. Cantelli, T. Autrey and M. A. Navarra, *J. Alloys Compd.*, 2011, **509**, S709.



- 25 Y. Filinchuk, A. Nevidomskyy, D. Chernyshov and V. Dmitriev, *Phys. Rev. B: Condens. Matter Mater. Phys.*, 2009, **79**, 214111.
- 26 J. Ross Macdonald, *LEVM version 8.0 Complex Nonlinear Squares Fitting Program*, 2003.
- 27 M. J. Frisch, G. W. Trucks, H. B. Schlegel, G. E. Scuseria, M. A. Robb, J. R. Cheeseman, G. Scalmani, V. Barone, B. Mennucci, G. A. Petersson, H. Nakatsuji, M. Caricato, X. Li, H. P. Hratchian, A. F. Izmaylov, J. Bloino, G. Zheng, J. L. Sonnenberg, M. Hada, M. Ehara, K. Toyota, R. Fukuda, J. Hasegawa, M. Ishida, T. Nakajima, Y. Honda, O. Kitao, H. Nakai, T. Vreven, J. A. Montgomery Jr., J. E. Peralta, F. Ogliaro, M. Bearpark, J. J. Heyd, E. Brothers, K. N. Kudin, V. N. Staroverov, R. Kobayashi, J. Normand, K. Raghavachari, A. Rendell, J. C. Burant, S. S. Iyengar, J. Tomasi, M. Cossi, N. Rega, N. J. Millam, M. Klene, J. E. Knox, J. B. Cross, V. Bakken, C. Adamo, J. Jaramillo, R. Gomperts, R. E. Stratmann, O. Yazyev, A. J. Austin, R. Cammi, C. Pomelli, J. W. Ochterski, R. L. Martin, K. Morokuma, V. G. Zakrzewski, G. A. Voth, P. Salvador, J. J. Dannenberg, S. Dapprich, A. D. Daniels, Ö. Farkas, J. B. Foresman, J. V. Ortiz, J. Cioslowski and D. J. Fox, *Gaussian 09, Revision D.01*, Gaussian, Inc., 2009.
- 28 Inorganic crystal structure database ICSD-164034.

